Equilibrium and Kinetic Properties of Triblock Copolymers at Hydrophobic Surfaces

Krister Eskilsson[†] and Fredrik Tiberg*[,‡]

Physical Chemistry 1, Chemical Center, Lund University, P.O. Box 124, S-221 00 Lund, Sweden, and Institute for Surface Chemistry, P.O. Box 5607, S-114 86 Stockholm, Sweden

Received December 4, 1996; Revised Manuscript Received July 2, 1997[⊗]

ABSTRACT: The adsorption of a series of (ethylene oxide−tetrahydrofuran−ethylene oxide), $EO_{n/2}THF_mEO_{n/2}$, triblock copolymers has been studied at the water/hydrophobic silica interface by time-resolved ellipsometry. The copolymers form monolayers with the middle tetrahydrofuran block anchoring at the surface and the ethylene oxide groups either anchoring at the surface or protruding into the aqueous phase. The degree of anchoring of the EO chains depends critically on the surface coverage. The copolymer isotherms are generally rather well described by the conventional Langmuir expression, and the plateau surface area per polymer molecule increases linearly with the molecular weight. However, the plateau thickness exhibits a more complex behavior. At low coverages, the adsorbed layer thickness is small, and both THF and EO chains form trains at the surface. As the surface coverage increases, however, the EO chains are increasingly forced away from the surface, and the mean thickness of the adsorbed layer exhibits a relatively strong linear dependence on the surface excess. At higher coverages, closer to the adsorption plateau, a weaker dependence is observed. The thickness increase is in this latter region due to the increasing steric repulsion between protruding EO chains. Outside the adsorbed layer, we also found support for the existence of a depletion layer. We show further that there are three regimes in the kinetics of adsorption. In the first (low surface coverage), the process is diffusion controlled and the rate is proportional to the concentration difference between the bulk solution and the subsurface located just outside the adsorbed layer. In the second regime (intermediate coverages and adsorption times), the kinetics are governed by the rate of displacement of anchored EO chains by THF chains of adsorbing copolymers. In the third regime (high surface coverages), the adsorption slows down markedly due to the energy barrier caused by presence of the relatively dense brush of adsorbed EO chains. In this regime, the surface excess varies proportionally with log t, which was also observed to be the case during the desorption process.

Introduction

Stabilization and flocculation of colloids, surface modification, and polymer compatibilization are all phenomena for which the interfacial behavior of adsorbed copolymers play a vital role (c.f. ref 1). Colloidal particles suspended in a liquid may for instance be protected from flocculation by surface anchored polymer chains when the free energy penalty of compressing the chains overcomes London−van der Waals attraction between dispersed particles. Important properties of interfacial copolymer layers for steric stabilization include the surface excess (grafting density) and the structure adopted by the copolymers at the surface as well as the kinetics of adsorption and desorption. The latter is important because equilibrium conditions are rarely fulfilled in practical applications. Large efforts have during many years been directed toward a better understanding of the adsorption behavior of block copolymers. A number of reviews and books have recently appeared in which this problem is discussed both from experimental and theoretical viewpoints.[2−6]

In this study, we report on the interfacial behavior of triblock copolymers at hydrophobized silica surfaces. The polymers consist of relatively small middle poly(tetrahydrofuran), PTHF, blocks that are capped by poly(ethylene oxide), PEO, chains at both ends. In aqueous solution, the PTHF blocks are preferentially adsorbed at the hydrophobic surface and the more water soluble PEO chains are to various extents protruding into the aqueous phase. These copolymers have previously not been studied, but there has been some work done on the adsorption of similar water soluble buoy−anchor−buoy, BAB, and anchor−buoy−anchor, ABA, copolymers at hydrophobic solid surfaces.[7−9]

Here, results on a series of $EO_{n/2}THF_mEO_{n/2}$ polymers with different block lengths are presented. In particular, we report on the adsorption isotherms, the concomitant evolution of the structure of the adsorbed layer, and the kinetics of adsorption and desorption. Furthermore, we point out the existence of a depletion region located between the adsorbed layer and the bulk solution. The observed structural properties are discussed on the basis of selected theoretical models for describing copolymer adsorption.[10,11] As a basis for interpretation of the kinetics, we use a model previously developed to describe the kinetics of surfactant adsorption and desorption.[12,13]

The adsorption is mainly studied by time-resolved ellipsometry, which is well suited for the attainment of an overall characterization of the interfacial properties of adsorbed layers of, e.g., copolymers and surfactants. It provides accurate measures of both layer thicknesses and adsorbed amounts with a good time resolution.

Experimental Section

Ellipsometry. The principles of ellipsometry are discussed extensively elsewhere.[14] In essence, the technique is used to measure polarization changes occurring at oblique reflection of a polarized light beam from a surface. The polarization changes are very sensitive to the presence of a thin film or a layer of adsorbed molecules at the surface. The difference in the polarization state between the incident and the reflected light is usually described by the measured parameters ψ and

[†] Lund University.
[‡] Institute for Surface Chemistry.
[⊗] Abstract published in *Advance ACS Abstracts,* September 1, 1997.

S0024-9297(96)01785-8 CCC: $14.00

Δ, often referred to as ellipsometric angles. These angles can by the following formula be expressed as functions of the wavelength of the light, λ, the angle of incidence, ϕ_0, and the optical properties of the reflecting system

$$\tan \psi \, e^{j\Delta} = f(\lambda, \phi_0, \text{optical parameters}) \qquad (1)$$

In the case of a reflection at one interface, the optical parameters are the refractive indices of the two phases. When planar, isotropic films are located between two bulk media, the overall reflection coefficients also depend on the thicknesses and refractive indices of each of these layers.[14]

The instrument used in this study was an automated Rudolph Research thin-film ellipsometer, type 43603-200E, equipped with high-precision step motors from Berger-Lahr, type VRDM 566, and controlled by a personal computer. The experimental setup as well as a description of the procedure for *in situ* characterization of thin films adsorbed on layered substrates are given in refs 15 and 13.

The systems discussed in this work were always treated as being composed of a number of homogenous and optically isotropic layers located between the substrate and the surrounding solution. All interfaces between these layers were assumed to be perfectly flat. The bulk silicon has a complex refractive index, $N_2 = n_2 - jk_2$, whereas both the silicon oxide and the adsorbed film are transparent (i.e. $k_i \approx 0$) and, thus, are characterized by thicknesses d_1 and d and the real parts of the refractive indices n_1 and n, respectively. A maximum of two of these parameters can be determined from a single set of ψ and Δ readings, provided that the rest of the parameters in eq 2 are known. All the measurements presented in this work were performed at $\lambda = 4015$ Å and $\phi_0 = 67°$.

In order to make accurate measurements of the adsorbed layer properties, knowledge of the substrate properties is required. Since four unknown parameters (n_2, k_2, n_1, and d_1) must be determined, at least four measured parameters are needed. For this purpose, a new methodology was developed, where two sets of ψ and Δ were determined in different ambient media (air followed by water). This substrate characterization procedure is described in refs 13 and 15. Typical values of n_2, k_2, n_1, and d_1 determined at $\lambda = 4015$ Å were $n_2 = 5.505 \pm 0.005$, $k_2 = -0.37 \pm 0.03$, $n_1 = 1.480 \pm 0.03$ and $d_1 \approx 300$ Å (varying somewhat between different substrate batches). As noted, we ignored the presence of the monomolecular hydrophobic film at the substrate surface (see below); i.e., an optical three layer model was used to characterize the substrate. This made the measurement procedure simpler, since measurements were only performed in two ambient media. Moreover, the error in the determined layer thickness caused by this simplification was found to be negligible.

When the optical properties of the substrate had been determined, a controlled amount of polymer was added to a temperature-controlled cuvette (25 ± 0.1 °C), and the ellipsometric angles ψ and Δ were then monitored as a function of time. Stirring was performed with a magnetic stirrer at about 300 rpm, and rinsing was done by a flow of DD-MP water through the cuvette. The maximum time resolution of our null ellipsometer is 1−2 s; however, to obtain high-precision measurements, we allowed approximately 3−4 s for measuring each set of ψ and Δ. Since the substrate properties were known, the average refractive index, n, and the mean thickness, d, of the adsorbed layer were calculated numerically from the ψ and Δ readings by a version of eq 1 derived for the optical four-layer model used to describe the system under study.[15] n and d were, as mentioned, calculated based on the assumption of adsorbed layer uniformity. For nonionic surfactants, it is observed that the thickness measured with ellipsometry agrees within a few ångström with the thicknesses obtained by neutron and X-ray scattering,[16−18] and neutron reflectivity,[19,20] as well as with PCS, streaming-potential measurements, and surface force measurements.[21,22] This indicates that the refractive index distribution within the adsorbed layer is relatively uniform, which further suggests that the mean optical thickness coincides reasonably well with the maximum extension of the adsorbed surfactant chains. However for polymer systems, d tends to represent the inner dense part of adsorbed polymer layers.[23,24]

Table 1. Molecular Weight of the Polymer, Number of Ethylene Oxide Groups, *n*, Number of Tetrahydrofuran Groups, *m*, and the Value of the Critical Micellar Concentration, Cmc

polymer	MW	*n*	*m*	cmc, wt %
P224-28	11900	224	28	0.03
P146-28	8400	146	28	0.04
P172-14	8600	178	14	0.2
P128-14	6700	128	14	0.15
P50-14	3200	50	14	0.02

The calculated values of n and d were also used to calculate the amount adsorbed or surface excess (Γ) according to the formula

$$\Gamma = \frac{(n - n_0)\, d}{\frac{dn}{dc}} \qquad (2)$$

where n_0 is the refractive index of the bulk solution ($n_0 = 1.3423 + C_b\,(dn/dc)$). dn/dc is the refractive index increment of the copolymers = 0.148 mL/g.

The effects of errors in the measured ellipsometric angles ψ and Δ on the calculated values of n and d were estimated earlier.[13] For typical experimental conditions, the errors in ψ and Δ are normally distributed with standard deviations of 0.001 and 0.002°, respectively. At small surface coverages, $\Gamma < 0.5$ mg m^{-2}, the relative error in the thickness is rather high; see ref 13. For larger adsorbed amounts ($\Gamma > 1$ mg m^{-2}), the errors rapidly decrease to values around 5−10%. The same trend was observed for the error in the refractive index. The errors in the adsorbed amount are much smaller. The maximum error in Γ in the low coverage limit, ≈0.1 mg m^{-2}, is about 15% and decreases to less than 1% for $\Gamma > 2$ mg m^{-2}. This is due to the fact that the errors in d and n are covariant in such a way that they to a large degree cancel out when Γ is calculated. Besides these errors, there are also systematic errors.[15] The effects of these have been discussed previously. Their magnitude was generally much smaller than the errors due to ψ and Δ fluctuations during the study of the adsorbed layer.

Materials. Five different (ethylene oxide−tetrahydrofuran−ethylene oxide) triblock copolymers, $EO_{n/2}THF_mEO_{n/2}$, have been studied in this work. Depending on the chemical composition, these are referred to as P224-28, P172-14, P146-28, P128-14, and P50-14, respectively (see Table 1), where the first number refers to the number of EO groups, n, and the second to the number of THF groups, m, of the polymer. The triblock copolymers were produced by Akzo Nobel Surface Chemistry, by ethoxylating different PTHF polymers with molecular weights of 1000 and 2000, respectively. The PTHF polymers were purchased from BASF. The average n/m ratio for the polymers were obtained from the NMR measurements, as the ratio between the integrals of the EO and THF signals, respectively. The measurements were performed on a Varian Unity 400 spectrometer equipped with a 360 MHz Oxford magnet. The molecular weight of each polymer was calculated from the n/m ratio and the known molecular weight of the PTHF block. The latter was taken as that stated by the manufacturer. A summary of the properties of the polymers used in this work is given in Table 1.

The polymer samples were before use extracted in a mixture of acetone and hexane in order to purify them from hydrophobic contaminants. To 15 g of polymer was added 50 cm^3 acetone, and the sample was then stirred for 15 min. Then, 150 cm^3 of hexane was added and the mixture stirred for another hour, and then the solvents were removed. This procedure was repeated five times. The aim of this washing step was to remove any hydrophobic contamination from the sample. After this extraction step, the polymers were dissolved in water and dialyzed against Millipore water. For this we used a Ultrasette from Filtron Technology Corp. with a

molecular weight cutoff of 3000. Finally, the polymers were freeze dried and stored in a refrigerator.

Cmc values were determined by the combined dye solubilization and absorption technique. For the absorption measurements, we used DPH (1,6-diphenyl-1,3,5-hexatriene) as a dye. The absorption was measured on a Parking Elmer UV−vis Lambda 14 spectrophotometer. A description of the experimental procedure is given in ref 25.

Polished silicon test slides (p-type, boron-doped, resistivity 1−20 Ω·cm) were purchased from Okmetic Ltd. The wafers were oxidized thermally in a saturated oxygen atmosphere at 920 °C for ≈1 h, followed by annealing and cooling in an argon flow. This procedure results in a SiO_2 layer thickness of ≈300 Å. The oxidized wafers were then cut into slides with a width of 12.5 mm and cleaned according to the procedure described in ref 15. The bare silica substrates were then treated in a plasma cleaner (Harrick Scientific Corporation, Model PDC-3XG) for 5 min just before use. These wafers were then placed in a reactor, which was evacuated by a water suction pump prior to the injection through a septum of 2 mL of dimethyloctylchlorosilane. The exposure to dimethyloctylchlorosilane was prolonged for about 18 h at 38 °C, and the wafers were then rinsed with ethanol followed by water, cleaned with surfactants, again rinsed in water and ethanol, and finally stored in ethanol. Before use, the surfaces were dried under vacuum, 0.001 mbar. To avoid potential problems associated with an air film sticking to the hydrophobic surface, ethanol was pumped through the cuvette before water was added. Note that reproducible measurements could not be obtained without this intermediate step. The ethanol was then rinsed of by a continuous flow of double distilled Millipore water, DD-MP, and prior to the start of the adsorption measurements, they were allowed to stabilize in the solvent for at least 1 h.

Rsults and Discussion

Using ellipsometry, we obtained independent time-resolved data on the surface excess, Γ, and the mean thickness, *d*, of the adsorbed layers of a series of $EO_{n/2}THF_mEO_{n/2}$ triblock copolymers at hydrophobized silica surfaces. The copolymers are here referred to as P*n-m* copolymers. The interfacial behavior of these polymers have to our knowledge not been investigated previously.

Before the adsorption behavior was studied, the polymers were characterized in terms of composition and molecular weights (see Table 1). In addition, the values of the critical micelle concentration, cmc, were determined by a dye solubilization and absorption technique. Previously, this method has been shown to give reliable measures of cmcs for (ethylene oxide−propylene oxide−ethylene oxide) triblock copolymers, the so-called Pluronics.[25] Figure 1 shows the absorbance, *A*, vs the bulk concentration, C_b, for the different $EO_{n/2}THF_mEO_{n/2}$ copolymers studied in this work. For a better overview, the concentration is given on a logarithmic scale. Due to polydispersity, the micellization process of copolymers is generally observed to proceeds over a rather broad concentration range. The cmcs obtained by the dye solubilization method are claimed to be indicative of the beginning of the micellization process, which is dominated by the aggregation of the least soluble copolymer fractions. The cmc's of the different copolymers are identified as the breakpoints of the $A-C_b$ curves in Figure 1 (see also Table 1). In agreement with the results by Alexandris *et al.*,[25] the cmcs of the P*n*-14 polymers were observed to increase with the hydrophilic-ethylene-oxide-to-hydrophobic-tetrahydrofuran ratio (*n*/*m*). However, the trend is not followed for the two P*n*-28 copolymers, but the values are rather close. This may be related to the polydispersity of the copolymers.

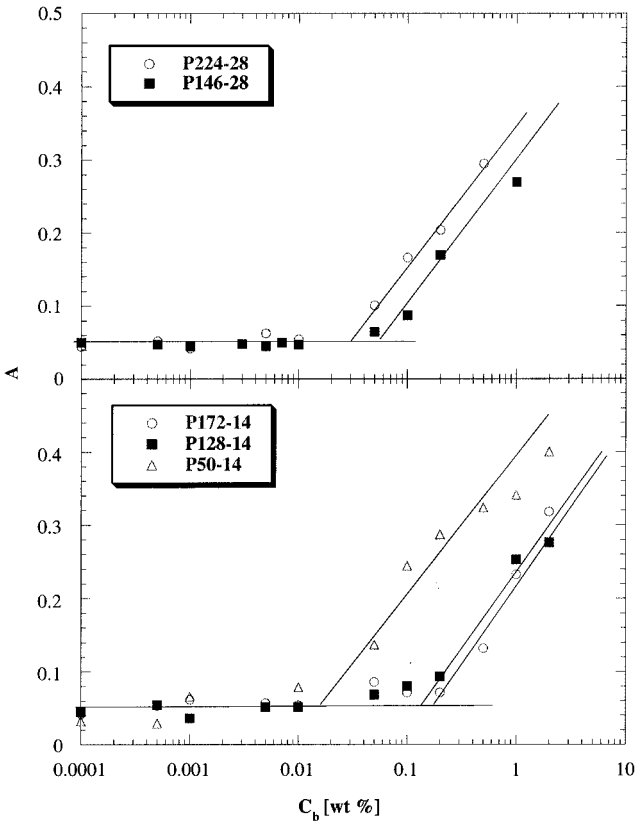

Figure 1. Absorbency vs concentration curves for the polymers P224-28, P146-28, P172-14, P128-14, and P50-14, respectively. The cmc's of the different polymers are identified as the breakpoints of the curves.

Adsorbed Amounts. We now turn our attention to the properties of these polymers adsorbed at hydrophobically modified silica surfaces. Figure 2 shows the isotherms for all the P*n-m* triblock copolymers studied. In all cases, the adsorption increases monotonously with the bulk copolymer concentration, C_b, until polymer concentrations in the region 0.1 to 1 cmc are reached. In this region, the adsorption levels off and relatively stable values are observed. This is a combined effect of the stabilization of the copolymer chemical potential near the cmc and the increased surface density of the adsorbed chains at the surface. It can also be seen in Figure 2 that the copolymer isotherms are rather well described by the simple Langmuir expression, having the general form

$$\Gamma = \frac{\Gamma_p C_b}{C_b + k} \tag{3}$$

where $k = k' \exp(\Delta\mu_{s-b}/k_bT)$. $\Delta\mu_{s-b}$ is the adsorption energy, $\mu_s - \mu_b$, and k' is a constant. Note that the rather stringent assumptions behind the Langmuir equation are not all fulfilled and therefore we chose not to discuss the magnitude of the fitted $\Delta\mu_{s-b}$ presented in Table 2. An interesting feature of the P*n-m* isotherms is that the plateau surface excess, Γ_p, is in the range of 2.3−2.5 mg m^{-2} for all copolymers. In fact, it is remarkably insensitive to the molecular weight and the chemical composition. Due to the hydrophobic nature of the middle THF block, we can assume that this interacts strongly with the hydrophobic surface. Figure 2 shows that a P90 homopolymer also adsorbs to the hydrophobic surface, but to a much smaller extent than the P*n-m* copolymers. In contrast to the copolymer

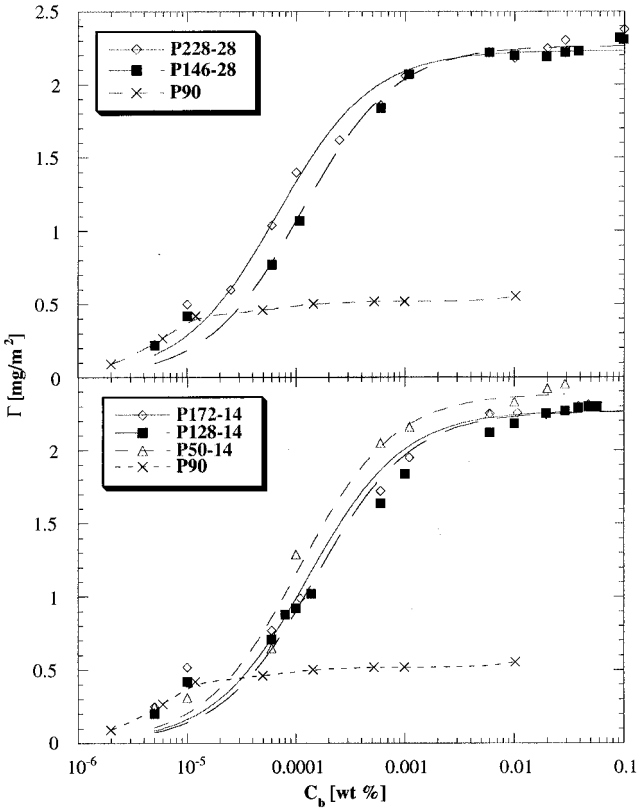

Figure 2. Adsorption isotherms for the homopolymer P90 and the copolymers P224-28, P146-28, P172-14, P128-14, and P50-14, respectively. The solid lines represent the best fit of the experimental copolymer isotherms to eq 3. The dashed line going through the data points of the P90 polymer is only drawn to guide the eye.

Table 2. Adsorbed Amount, Γ_p, Adsorbed Layer Thickness, d_p, Volume Fraction of Copolymer in the Adsorbed Layer, ϕ_p, Reduced Coverage, and the Adsorption Energy per Molecule, $\Delta\mu_{s-b}$, Respectively[a]

polymer	Γ_p, mg m^{-2}	d_p, Å	ϕ_p, vol %	$2\pi R_g^2/\Sigma_p$	$\Delta\mu_{s-b}$, kT
P224-28	2.4	60	0.2	6.5	−13.8
P146-28	2.3	34	0.6	6.7	−13.0
P172-14	2.3	47	0.25	5.5	−12.7
P128-14	2.3	37	0.3	6.5	−12.5
P50-14	2.4	30	0.5	5.3	−12.9

[a] Subscript p denotes plateau values.

isotherms, the P90 homopolymer isotherm is of the typical high-affinity type common for long-chain polymers. A reflection of this behavior is also seen at low polymer concentration in the copolymer isotherms. It appears as if the end-blocks dominate the adsorption at low bulk copolymer concentrations; i.e., the copolymers behave as PEO homopolymers in this concentration region. As is seen in Figure 2, the surface excess in the low concentration regime increases with increasing molecular weight. At slightly higher concentrations, the surface excess begins to increase for all copolymers, reflecting the presence of the more hydrophobic PTHF segments. In this second concentration regime, all isotherms exhibit a similar Langmuir-type evolution, although the increase of Γ with C_b for copolymers with the longest PEO chains tends to be somewhat smaller than expected from the theoretical Langmuir curves. To summarize, at low surface coverage the copolymers forms a mixed pancake of PTHF and PEO segments, and the surface excess depends on the copolymer molecular weight in a fashion resembling that observed

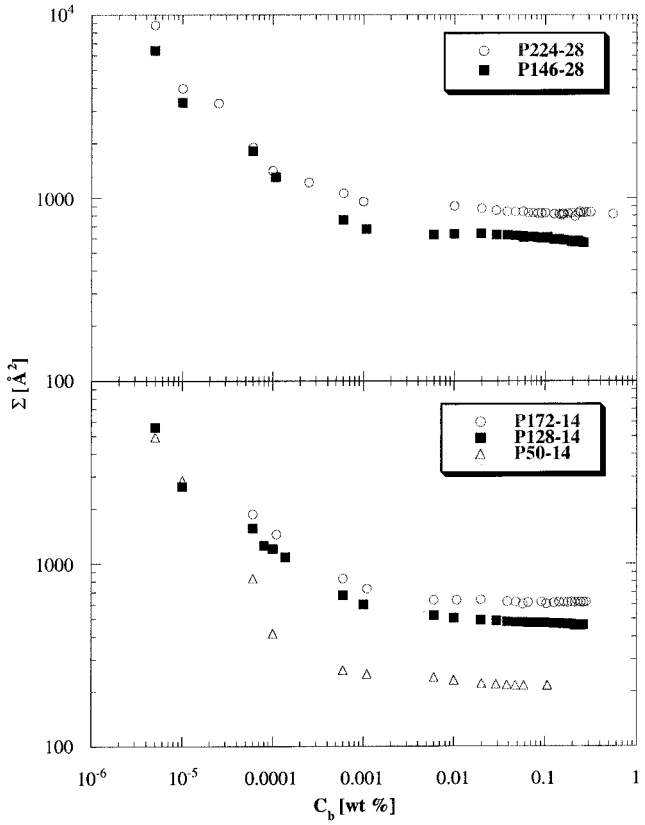

Figure 3. Area per molecule vs the bulk concentration for the copolymers P224-28, P146-28, P172-14, P128-14, and P50-14, respectively.

for homopolymer PEOs.[26] At higher concentrations the PEO trains are increasingly replaced by a PTHF train and therefore stretch out from the surface. This behavior is discussed below.

The area per polymer molecule, Σ, as a function of the bulk concentration of the different copolymers is shown in Figure 3. Before the plateau values are reached, the area decreases as the bulk concentration increases. The data also shows that the smallest plateau areas are obtained for the smallest copolymer. Figure 5a shows further that the plateau surface area per polymer molecule, Σ_p, increases linearly with the molecular weight, MW, of the copolymer. The dependence of Σ_p on the number of EO and THF groups, respectively, is therefore similar. We have compared this observation with data extracted from adsorption studies of different Pluronic system on polystyrene by Baker and Berg (latex particles)[27] and on hydrophobized silica by Steeg and Gölander.[28] We also used data presented by Pai−Panadiker and co-workers on triblock copoly(styrene−ethylene oxide) adsorbed on silica.[29] For all these systems, we also found linear relationships between Σ_p and MW.

Marques, Joanny, and Leibler (MJL) formulated a scaling description of the adsorption of diblock copolymers at surfaces from selective solvents,[11] which in some previous studies has been shown to describe equilibrium properties of adsorbed copolymer layers rather well.[30−32] MJL found two different scaling regimes depending on the relations between the size of the anchoring and buoy segments. The asymmetry ratio β_s ($=N_A^{-1/2}N_B^{3/5}a$) determines which scaling relation is applicable for a certain copolymer system. Here, the constant a gives the ratio between buoy and anchor monomer sizes. When β_s is approximately equal to unity, MJL predicted

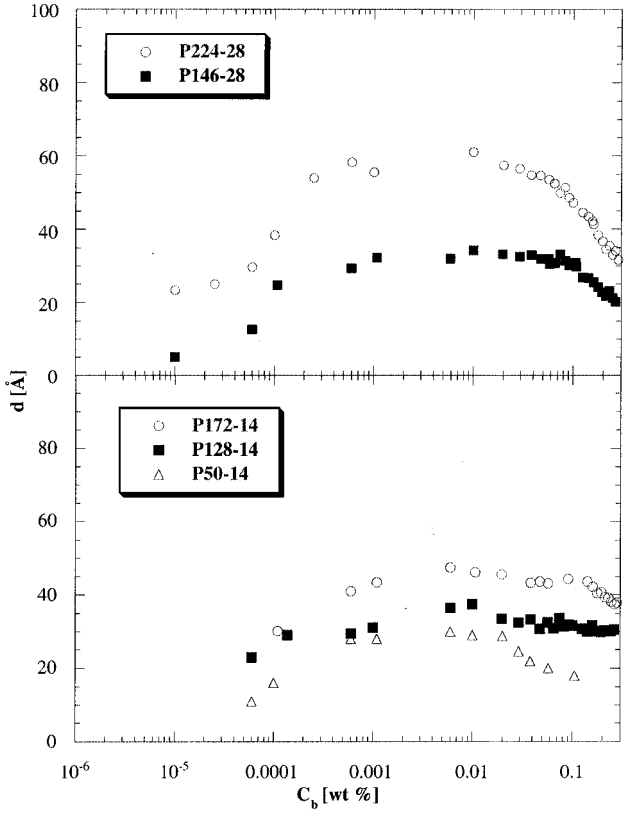

Figure 4. Mean adsorbed layer thickness vs bulk concentration for the copolymers P224-28, P146-28, P172-14, P128-14, and P50-14, respectively.

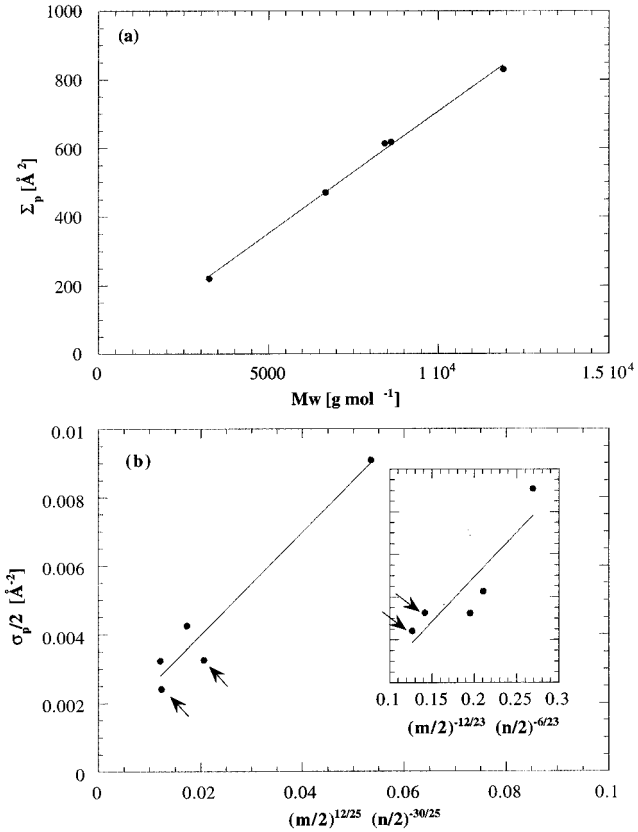

Figure 5. (a) Plateau values of the surface area (Σ_p) per copolymer vs the molecular weight. (b) Plateau values of the copolymer surface density per every half triblock copolymer ($\sigma_p/2$) vs $(m/2)^{-12/23}(n/2)^{-6/23}$ in the main graph, and $(m/2)^{12/25}(n/2)^{-30/25}$ in the insert, respectively (see also the Discussion). Solid lines represent the best linear fits to the experimental data. The results for P*n*-28 copolymers are marked with arrows.

that the plateau surface density per molecule, σ_p (=1/Σ_p), should follow a $\sigma_p \sim N_A^{12/25}N_B^{-30/25}$ scaling law, whereas a $\sigma_p \sim N_A^{-12/23}N_B^{-6/23}$ relation should be obeyed when β_s is much larger than one. These two regimes were referred to as the van der Waals (vdW)−brush regime and the buoy-dominated regime, respectively. The properties of the adsorbed layer are in the vdW−brush regime determined by the balance between van der Waals interaction between the anchor segments and the surface, on the one hand, and the stretching energy of the buoys, on the other, whereas the stretching of the buoys is responsible for the layer structure in the buoy-dominated regime. The theory of MJL was developed for diblock copolymers and has yet to be extended to triblock copolymer systems. However, we can assume that our triblock copolymer are composed of two diblock copolymers with $m/2$ anchoring THF monomers and $n/2$ EO buoy segments, respectively.

In Figure 5b, we have plotted $\sigma_p/2$ vs both $(m/2)^{-12/23}(n/2)^{-6/23}$ and $(m/2)^{12/25}(n/2)^{-30/25}$. As is seen, our results do not appear to be in very good agreement with the predictions by the MJL theory. This can be due to the fact we are dealing with triblock copolymers instead of diblocks, which the theory was developed for. The solvent selectivity may also not be large enough. Indeed, PEO is not in good solvency conditions in water.[6] Perhaps more important, however, is the fact that the asymmetry ratio for all copolymers is between one and four and, hence, in a region where the contribution of vdW interactions and chain stretching is not clear-cut. In fact an intermediate and, hence, small scaling of $\sigma_p/2$ with $m/2$ gives a good fit with our experimental results. It is further noted that the molecular weights of our copolymers vary by less than an order of magnitude, which makes it difficult to evaluate scaling dependences.

The reduced coverage at plateau conditions, $2\pi R_g^2/\Sigma_p$, where R_g is the radius of gyration of one unperturbed $EO_{n/2}$ chain in solution, tells us how packed the individual EO chains are in the adsorbed layer at plateau conditions. The reduced surface coverage is for these copolymers between 5 and 7 (see Table 2), indicating that the EO chains are stretched at plateau adsorption conditions but that the asymptotic brush limit is not reached. This occurs at $2\pi R_g^2/\Sigma_p > 12$.[33,34] The values reached in this study are typical for physically adsorbed copolymers. The values of R_g for the ethylene oxide chains were obtained from a rheological study performed by Bhat and Timasheff.[35]

Layer Thicknesses. Figure 4 shows the adsorbed layer thickness plotted against the bulk concentration. For all P*n*-*m* copolymers studied, the thickness increases monotonously with the concentration until a pseudoplateau is reached (see below). The small thicknesses observed at low copolymer concentrations and surface coverage indicate that the polymers in this region adopt a relatively flat configuration normal to the surface with a large number of copolymer segments forming trains. The relatively small thickness agrees well with the above discussion of the structural evolution with the surface coverage. As the surface coverage increases, the adsorbed layer thickness increases with an increment that is highly dependent on the number of EO groups of the copolymer, n. Below approximately 1−1.5 mg m^{-2}, the increase of d with Γ is more rapid

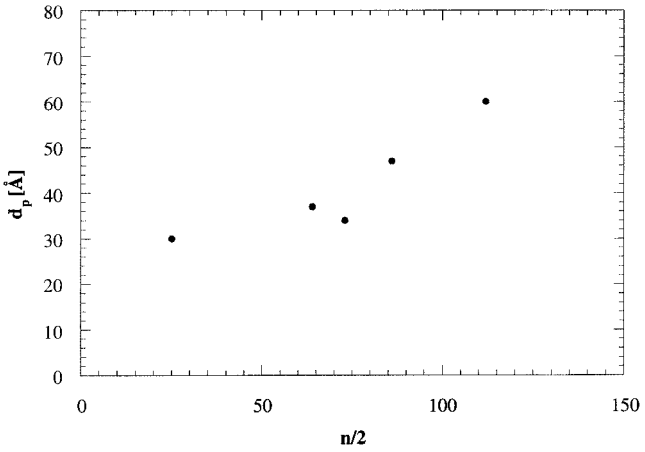

Figure 6. Mean thickness at the pseudoplateau plotted as a function of the number of EO groups in the end blocks.

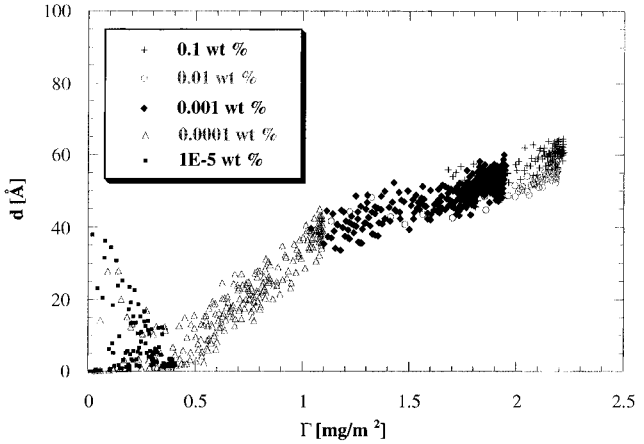

Figure 7. Mean thickness vs the surface excess. The data summarizes five kinetic measurements performed at five different P224-28 bulk concentrations.

than at higher Γ values (see Figures 2 and 4). The larger increase in the adsorbed layer thickness with increasing C_b in the low surface coverage regime is believed to be a consequence of a steady decrease of the number of EO trains at the surface. However, above a certain surface coverage, essentially no EO trains are present at the surface. The thickness increase is in this region is a result of the stretching of the EO chains caused by their mutual repulsive interactions. A much weaker dependence is observed in the high surface coverage region. Figure 7 shows this evolution very nicely. The graph shows the dependence of the mean thickness, d, on the surface excess, Γ, where the data has been collected from five time-resolved measurements of d and Γ performed at five different bulk concentrations of P224-28 (see below). The majority of the data shown are collected during slow adsorption ($\ll$0.001 mg/m^2 s). The curve confirms the above discussed structural evolution, where the polymer initially is adsorbed in a flat conformation with both PEO and PTHF segments in train configurations. As the coverage increases, PEO is increasingly forced away from the surface and finally the thickness increase is only a result of stretching of EO chains due to steric repulsive interactions betweeen the chains. A sketch of this evolution is shown in Figure 8. This interpretation is supported by the observed adsorption kinetics discussed later in this paper. This pancake to brush transition was theoretically predicted by Alexander.[10] He showed that for copolymers with buoys that have a

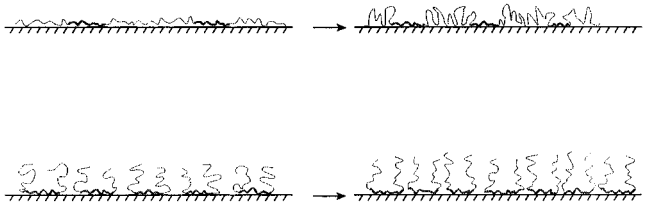

Figure 8. Sketch of the evolution of the copolymer conformations in the adsorbed layer with increasing surface coverage.

finite affinity (although still soluble) for the surface, a transition occurs at a critical surface concentration. The polymers transform from a uniform adsorption to a polar head configuration (brush configuration). This transition has been experimentally observed for triblock and diblock copolymers at both the air−liquid and solid−liquid interfaces.[36,9]

The value of the thickness at the semiplateau, d_p, is shown in Figure 6 and Table 2. With the exception of the smallest P50-14 polymer, d_p scales with the number of EO groups according to the approximate relation $d_p \propto n$. Unfortunately, it is difficult to compare our data with theory because the ellipsometric thickness differs from the hydrodynamic thickness determined in most theoretical studies; cf. refs 10, 11, and 37. The ellipsometric thickness represent an average thickness calculated under the assumption of layer uniformity. For adsorbed surfactants, this coincides well with the extension of the adsorbed layer, whereas for homopolymers it does not. It is shown by de Gennes that the ellipsometric thickness for adsorbed homopolymers scales with the number of monomers to the power 0.4.[23] The corresponding scaling factor for the hydrodynamic thickness is 0.6. If the functional form of the segment density profile is known and if this is a two-parametric function, then these can be obtained by fitting to the ellipsometric data. A combination of thickness measurements can be used to get information about the segment density profile. The present study will be extended to light scattering and neutron reflectivity measurements. However, at present we conclude that, with the exception of the smallest copolymer, the ellipsometric thickness appears to follow a linear relation with the number of ethylene oxide groups.

Using the adsorbed layer thickness at the semiplateau and the molecular volumes of the polymers, the mean ellipsometric copolymer volume fraction in the adsorbed layer, ϕ_p, was calculated (see Table 2). For polymers with constant PTHF size, ϕ_p, decreases strongly when the number of EO monomers increases, i.e., reflecting the increasing steric repulsive interactions between EO chains on increasing the EO chain length.

Depletion Layers. The adsorbed layer thicknesses measured above approximately 0.01 wt % are not believed to be physically correct. The decreasing trend observed in this region is instead believed to be the consequence of a depletion layer located outside the adsorbed layer. The reason for this suggestion is that the decrease of the thickness is observed in the concentration region where the optical contrast between a depleted layer and the bulk solution becomes significant and the cmc is exceeded. The presence of such a layer would result in a lowering of the thickness calculated by the optical four-layer model used for interpreting the data. By assigning a constant adsorbed layer thickness value equal to that observed at the semiplateau, it is possible to calculate the depletion layer thickness using an optical five-layer model. This is a fairly good approximation, since the osmotic pressure exerted by

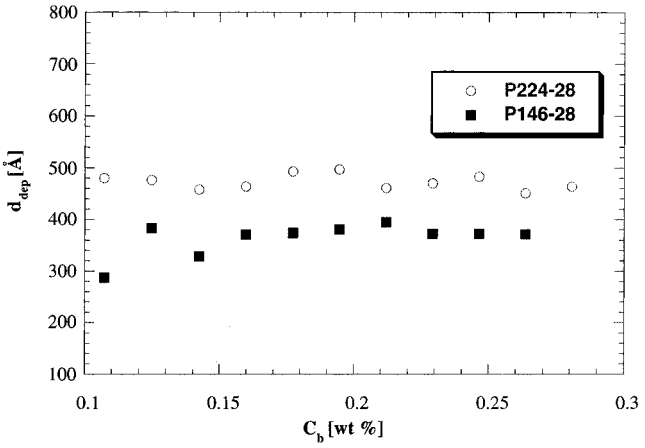

Figure 9. The depletion layer thickness of P-224-28 and P146-28 calculated under the assumption of constant adsorbed layer thickness using a five-layer optical model.

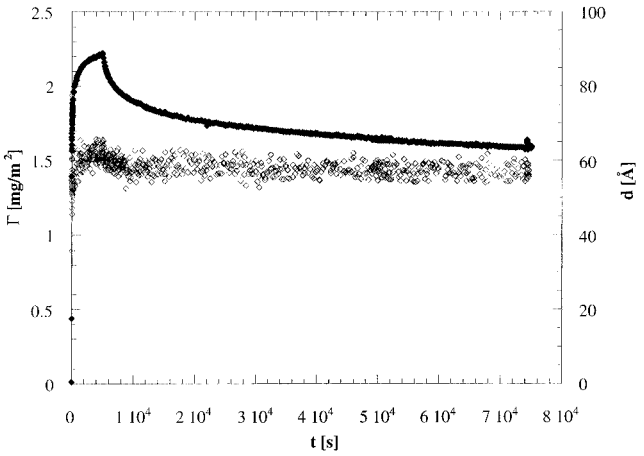

Figure 10. Time-dependence of the surface excess and the adsorbed layer thickness measured during adsorption and desorption of P224-24. The copolymer was injected at $t \approx 0$ ($C_b = 0.01$ wt %) and rinsing with pure water was initiated at $t \approx 5000$ s.

the bulk solution is relatively small at these bulk concentrations. In Figure 9, we only show the values for the P*n*-28 copolymers for which the effect is most clear. The thicknesses of the depletion layers obtained with the above assumptions is, as can be seen, fairly constant with increasing bulk concentration. Only a slight decrease is observed with increasing polymer bulk concentration, C_b. This could mirror a decreasing thickness of the adsorbed and/or depleted layers due to the increasing osmotic pressure. Note that the data in Figure 9 are based on many assumptions, and therefore the absolute value of the depletion layer thickness may not be entirely adequate; however, the presence of a depleted layer outside the adsorbed layers appears clear.

Adsorption and Desorption Kinetics. Most of the kinetic data presented in this part features P228-28, which is the copolymer studied most extensively in this investigation. Figure 10 shows the time dependence of the surface excess and the adsorbed layer thickness measured during adsorption and desorption for P224-28. The polymer is injected at $t = 0$ ($C_b = 0.01$ wt %). The initial adsorption at this concentration is fast. With increasing time and surface coverage, the rate slows down markedly. As the adsorption stabilizes, rinsing with pure water is initiated. At the beginning of the rinsing process, desorption proceeds relatively rapidly, but the rate of this process slows down with time and

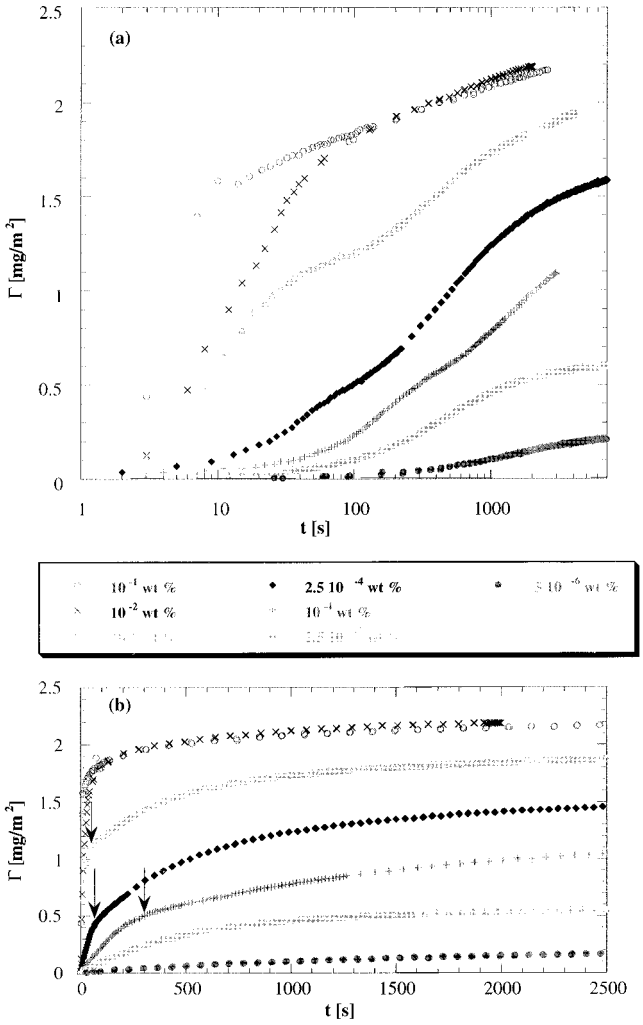

Figure 11. Time-dependence of the surface excess during adsorption of P224-24 from solutions with different bulk concentrations ranging from 5×10^{-6} to 0.1 wt %. Graph a shows the measured data on a lin−log scale whereas b shows a close up of the data on lin−lin scale. The arrows indicate for a few clear cases approximately when the substitution controlled regime is first encountered.

the total faction of polymers desorbed during the first 20 h is only about 25%. The copolymers may therefore be viewed as irreversibly adsorbed in most practical applications or at least in those in which no displacers are used. Parts a and b of Figure 11 show series of time-resolved adsorption measurements performed for the same P224-28 copolymer at different bulk concentrations. For the sake of clarity, we chose to plot the curves on a linear as well as a logarithmic scale. This first encountered adsorption regime represents the beginning of the diffusion-controlled regime which is prevalent at low surface coverages and short times. In addition to this, a chain substitution regime is identified at intermediate coverages and intermediate times. In Figure 11b, the start of this regime is identified by arrows. Finally an activation barrier controlled regime is also observed at high coverages and long times. We will now look into these regimes a bit more closely.

In previous articles, we have used the simplified picture of a stagnant layer with a finite thickness δ to describe the diffusion path from the bulk solution to the surface.[12,13] This was found to be useful for describing and predicting the adsorption kinetics of surfactant systems. The transport rate of the copolymers through

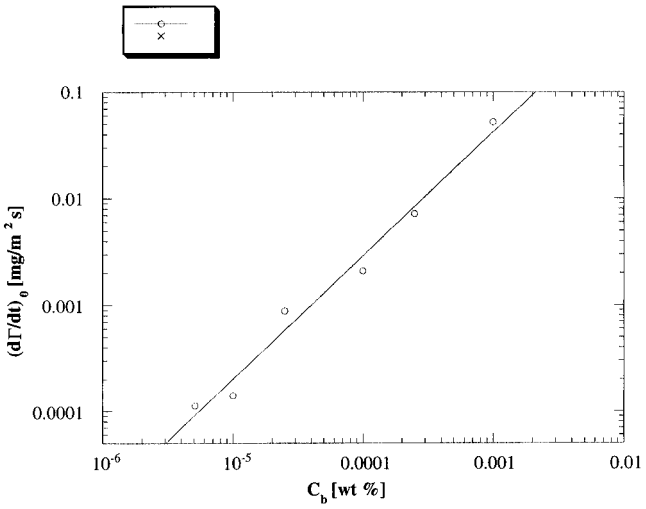

Figure 12. Inital adsorption rate vs the bulk concentration of P224-24 plotted on a log−log scale.

the stagnant layer is given by

$$\frac{d\Gamma}{dt} = \frac{D_p}{\delta}(C_b - C_s(\Gamma)) \quad (4)$$

where D_p is the copolymer diffusion coefficient and $C_s(\Gamma)$ is the surface concentration at a particular Γ. Here, we only deal with copolymer concentrations below the cmc.

The adsorption rates in the diffusion-controlled regime can be predicted from the isotherm. Assuming fast equilibration in the surface region, the concentration of copolymer in the immediate vicinity of the adsorbed layer, $C_s(\Gamma)$, at a particular Γ value is equal to the inverse isotherm $C_b(\Gamma)$. $C_b(\Gamma)$ can be directly obtained from eq 3, if the factual deviations from the Langmuir isotherm are ignored. The following expression for the adsorption rate is then obtained under steady-state conditions:

$$\frac{d\Gamma}{dt} = \frac{D_p}{\delta}\left(C_b - \frac{k\Gamma}{\Gamma_p - \Gamma}\right) \quad (5)$$

In the very beginning of the adsorption process, the adsorption rate should be proportional to C_b. This is shown in Figure 12, where the initial adsorption rate is plotted against the bulk copolymer concentration on a double logarithmic scale. We have previously found that δ is about 1×10^{-4} m. Using this value and the slope of the power law fit in Figure 11, D_p was estimated to be $(4 \pm 1) \times 10^{-10}$ m^2 s^{-1}. This is in the right ballpark. FT-PGSE NMR measurements show that D_p determined at 0.05 wt % is $\approx(2 \pm 1) \times 10^{-10}$ m^2 s^{-1}. Unfortunately, measurements could not be performed at lower concentrations due to the large signal to noise ratio. D_p is, however, expected to increase with decreasing concentration, if the observed trend in the NMR data in interval 5−0.05 wt % continues. The time dependence of adsorption in the diffusion controlled regime can be obtained from eq 5. Integrating this equation from $t = 0$, $\Gamma = 0$ to t, Γ, we find

$$\frac{\Gamma_p}{k + C_b}\left(\frac{\Gamma}{\Gamma_p} - \frac{k}{k + C_b}\ln\left(1 - \frac{k + C_b}{C_b}\frac{\Gamma}{\Gamma_p}\right)\right) = \frac{D_p}{\delta}t \quad (6)$$

This relation describes rather well the adsorption curves at low surface coverages (see examples in Figure 13).

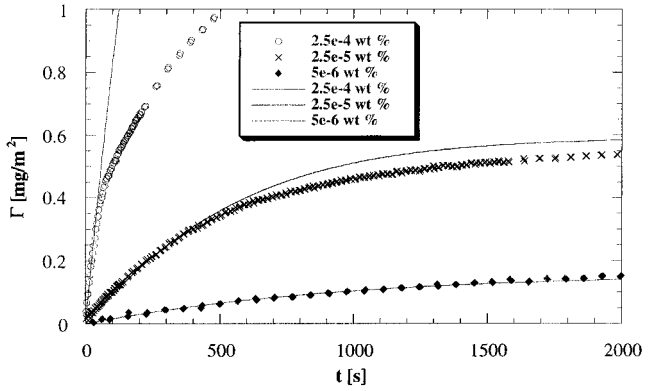

Figure 13. Surface excess vs time during adsorption from P224-28 solutions of different bulk concentrations. The solid lines are theoretical curves according to eq 6. The values used for k and Γ_p were the same as those obtained from the fit of eq 3 to the isotherm. D_{mon} is estimated to be $4 \pm 1 \times 10^{-10}$ m^2/s, when δ was taken to be the value obtained in ref 12, i.e., 10^{-4} m).

Deviations from the theoretical relation can be an effect of copolymer polydispersity as well as the use of the Langmuir expression for the experimental isotherm.

In the substitution regime, appearing at intermediate times and surface coverages, the adsorption increases close to linearly with time, but with a slower rate than predicted by eq 5. The presence of this regime is particularly clear in curves measured in the region $10^{-4} \geq C_b \geq 10^{-2}$ wt %; see Figure 11b. The transition to the substitution-controlled regime is indicated by arrows. It is inferred that the rate-determining step in this regime is the detachment and subsequent substitution of anchored EO chains by THF chains of adsorbing copolymers. At these intermediate concentrations, the adsorption is sufficiently slow for the EO chains to attach to the surface, and the final surface coverage is large enough for the substitution process to take place at intermediate coverages. This is further supported by the fact that the approximate Γ value where the substitution regime is observed coincides with the region in the d(Γ) curve where the thickness rapidly increases with the surface coverage, i.e., Γ between approximately 0.5 mg m^{-2} and 1.2 mg m^{-2} (see Figure 6). Moreover, during fast adsorption processes (observed during adsorption from solutions with high C_b) this regime is not encountered. Figure 14 shows the adsorption kinetics for all P*n*-*m* copolymers studied. To make comparisons easy, all measurements were performed at the same molar bulk concentration, and the surface excess is given in μmol m^{-2}. We chose a bulk concentration in the interval where the presence of the substitution regime is observed clearly for all copolymers, $C_b = 0.21$ mol m^{-3}, and the polymers have a relatively slow adsorption and hence time to adjust to a close to equilibrium conformation. As expected, the adsorption of the different P*n*-*m* copolymers initially exhibits the same time dependence. The surface coverage at which deviations from the diffusion limited regime are first observed and the substitution limited regime is encountered increases with decreasing MW or *n* value of the copolymer. Figure 15 shows the area per adsorbed P*n*-*m* molecule at this transition, Σ_{d-s}, plotted vs the molecular weight of the copolymer, MW. Σ_{d-s} shows a linear dependence on MW, i.e. following the same relation as the plateau area per copolymer molecule. Interestingly, the reduced surface coverage at the transition, $2\pi R_g^2/\Sigma_{d-s}$, is for all copolymers approximately 1.5, i.e. substitution begins at a packing density

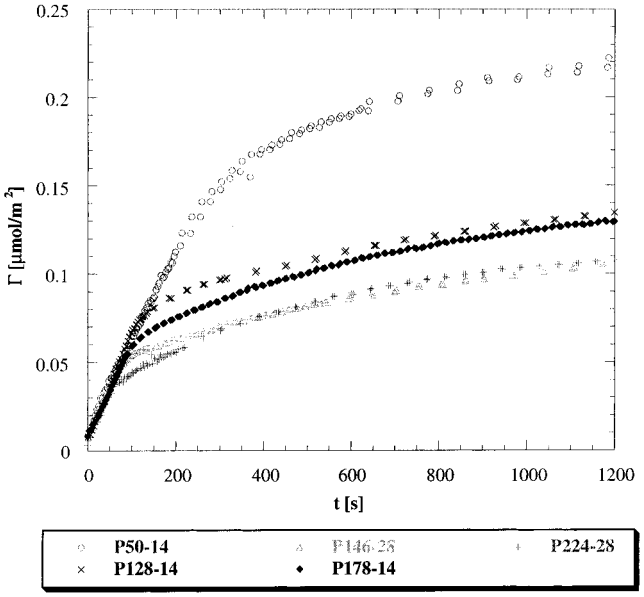

Figure 14. Surface excess vs time for P224-28. P146-28, P178-14, P128-14 and P50-14, respectively. All adsorption measurements are performed at $C_b = 2.1 \times 10^{-5}$ mol/m^3 and the surface excess is given in μmol/m^2. This is done to make comparison of the data easier.

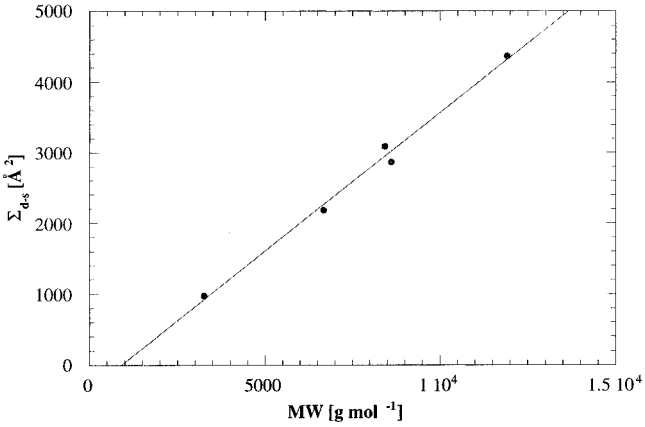

Figure 15. Surface area per EO chain at the break between the diffusion controlled and the substitution-controlled regimes measured at 2.1×10^{-1} mol/m^{-3}. Also shown are the calculated equator area of a PEO chain vs the number of monomers in the chain. The values of the radius of gyration for the latter were taken from ref 35.

just above that when undisturbed chains in solution start to interact. $2\pi R_g^2/\Sigma_{d-s} \approx 1.5$ is also where the thickness begins to increase linearly in Figure 6. It is clear that the rate in the substitution limited regime must be proportional to adsorption energies of the PEO and PTHF segments, respectively. We have at present no theory describing the rates in the substitution regime. More theoretical and experimental work is, however, needed for a better understanding of the kinetics displayed in this regime. Note, finally, that the reduced surface coverage at which the diffusion limited regime ends increases when the copolymer adsorption rate increases (see Figure 11b). This is consistent with the fact that the EO chains have shorter and shorter time to relax at the surface. At even faster adsorption, a direct transition from diffusion to barrier limited adsorption is observed.

In this final regime (at high surface coverages or long times for intermediate surface coverages), a logarithmic time dependence of Γ is observed; see Figures 11 and 16. We infer that the kinetics in this region is controlled by an activation barrier caused by overlapping and stretching EO chains. Theoretical studies performed by Ligoure and Leibler as well as Johner and Joanny are in qualitative agreement with our experimental data in the high surface coverage region.[38,39] In these studies, it is pointed out that the surface coverage of end-adsorbing chains should (as we observe) increase slowly (logarithmic) with time in the brush-dominated regime. However, a quantitative interpretation of our data using their respective theories is difficult due to their simplified approach to the kinetic problem and differences in the systems studied.

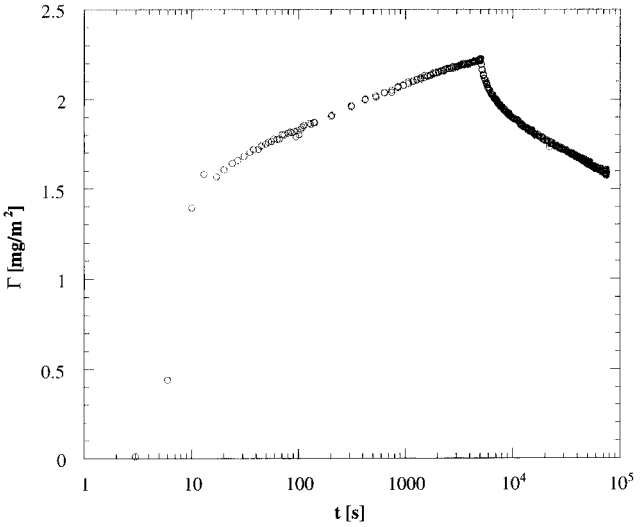

Figure 16. Surface excess vs time from Figure 8, but on a lin−log scale.

Figures 11 and 16 also show the desorption kinetics. Again the surface excess varies linearly with log(t). Due to the slow kinetics, we have only followed this process partly. The time required for complete desorption would be about 2000 years, if the same time dependence would prevail during the whole desorption process. Interestingly, the absolute increment with log(t) is almost the same during adsorption and desorption. Ligoure and Leibler pointed out that the time to "wash off" an adsorbed brush with fresh solvent would be much longer than the characteristic time required to grow the brush.

Acknowledgment. We thank Professor Martin Heusten (Akzo Nobel Surface Chemistry AB) for providing the polymer samples used in this study. The Swedish National Board for Industrial and Technical Development (NUTEK) and the Swedish Research Council for Engineering Sciences (TFR) are acknowledged for financial support.

References and Notes

(1) Napper, D. H. *Polymeric Stabillization of Colloidal Dispersions*; Academic Press: London, 1983.
(2) de Gennes, P. G. *Adv. Colloid Interface Sci.* **1987**, *27*, 189.
(3) Halperin, A.; Tirell, M.; Lodge, T. P. *Adv. Polym. Sci.* **1992**, *100*, 31−72.
(4) Whitmore, M. D.; Noolandi, J. *Macromolecules* **1990**, *23*, 3321−3339.
(5) Milner, S. T. *Science* **1991**, *21*, 905−914.
(6) Fleer, G. J.; A., C. S. M.; Scheutjens, J. M. H. M.; Cosgrove, T.; Vincent, B. *Polymers at Interfaces*, 1st ed.; Chapham & Hall: London, 1993.
(7) Jiang, Q.; Chiew, Y. C.; Valentini, J. E. *Colloids Surf. A* **1996**, *113*, 127−134.
(8) Tiberg, F.; Malmsten, M.; Linse, P.; Lindman, B. *Langmuir* **1991**, *7*, 2723.

(9) Ou-Yang, D. H.; Zihao, G. *J. Phys.* **1991**, 1375−1385.
(10) Alexander, S. *J. Phys.* **1977**, *38*, 983−987.
(11) Marques, C.; Joanny, J. F.; Leibler, L. *Macromolecules* **1988**, *21*, 1051−1059.
(12) Tiberg, F.; Jönsson, B.; Lindman, B. *Langmuir* **1994**, *10*, 3714.
(13) Tiberg, F. *J. Chem. Soc., Faraday Trans.* **1996**, *92*, 531.
(14) Azzam, R. M. A.; Bashara, N. M. *Ellipsometry and Polarized Light*; North Holland: Amsterdam, 1989.
(15) Tiberg, F.; Landgren, M. *Langmuir* **1993**, *9*, 927.
(16) Cummins, P. G.; Staples, E.; Penfold, J. *J. Phys. Chem.* **1991**, *95*, 5902.
(17) Cummins, P. G.; Staples, E.; Penfold, J. *J. Phys. Chem.* **1990**, *94*, 3740.
(18) Gellan, A.; Rochester, C. H. *J. Chem. Soc., Faraday Trans. 1* **1985**, *81*, 2235.
(19) McDermott, D. C.; Lu, J. R.; Lee, E. M.; Thomas, R. K.; Rennie, A. R. *Langmuir* **1992**, *8*, 1204.
(20) Lu, J. R.; Li, Z. X.; Su, T. J.; Thomas, R. K.; Penfold, J. *Langmuir* **1993**, *9*.
(21) Böhmer, M. R.; Koopal, L. K.; Janssen, R.; Lee, E. M.; Thomas, R. K.; Rennie, A. R. *Langmuir* **1992**, *8*, 2228.
(22) Tiberg, F.; Ederth, T.; Claesson, P. Work in progress.
(23) de Gennes, P. G. Polymer Adsorption. In *Liquids at Interfaces*; Charvolin, J., Joanny, J. F., Zinn-Justin, J., Eds.; North Holland: Amsterdam, 1990.
(24) Rivory, J.; Frigerio, J. M.; Marques, C. *Opt. Comm.* **1992**, *89*, 482.
(25) Alexandridis, P.; Holzwarth, J. F.; Hatton, T. A. *Macromolecules* **1994**, *27*, 2414−2425.
(26) Trens, P.; Denoyel, R. *Langmuir* **1993**, *9*, 519.
(27) Baker, J. A.; Berg, C. J. *Langmuir* **1988**, *4*, 1055−1061.
(28) van de Steeg, L. M. A.; Gölander, C.-G. *Colloids Surf.* **1991**, *55*, 105−119.
(29) Pai-Panandiker, R. S.; Dorgan, J. R.; Carlin, R. T.; Uyanik, N. *Macromolecules* **1995**, *28*, 3471.
(30) Hadziioannou, G.; Patel, S.; Granick, S.; Tirell, M. *J. Am. Chem. Soc.* **1986**, *108*, 2869−2876.
(31) Parsonage, E.; Tirrell, M.; Watanabe, H.; Nuzzo, R. G. *Macromolecules* **1991**, *24*, 1987−1995.
(32) King, M. S.; Cosgrove, T.; Eaglesham, A. *Colloids Surf. A* **1996**, *108*, 159−171.
(33) Baranowsky, R.; Whitmore, M. D. *J. Chem. Phys.* **1995**, *6*, 2343.
(34) Kent, M. S.; Lee, L. T.; Factor, B. J.; Rondelez, F.; Smith, G. S. *J. Chem. Phys.* **1995**, *103*, 2321−2341.
(35) Bhat, R.; Timasheff, S. N. *Protein Sci.* **1992**, *1*, 1133−1143.
(36) Bijsterbosch, H. D.; de Haan, V. O.; de Graaf, A. W.; Mellema, M.; Leermakers, F. A. M.; Cohen Stuart, M. A.; van Well, A. A. *Langmuir* **1995**, *11*, 4467.
(37) Milner, S. T.; Witten, T. A.; Cates, M. E. *Macromolecules* **1988**, *21*, 2610−2619.
(38) Ligoure, C.; Leibler, L. *J. Phys. Fr.* **1990**, *51*, 1313.
(39) Johner, A.; Joanny, J. F. *Macromolecules* **1990**, *23*, 5299−5311.

MA961785P